

Theoretical investigation of monolayer MoS₂ on oxide

Amithraj Valsaraj^a, Jiwon Chang^b, Leonard F. Register^a and Sanjay K. Banerjee^a

^aMicroelectronics Research Center, The University of Texas at Austin, Austin, TX-78758, USA

^bSEMATECH, 257 Fuller Rd #2200, Albany, NY-12203, U.S.A

Monolayer transition metal dichalcogenides are novel, gapped two-dimensional materials. Toward device applications, we study the effect of dielectric oxide slabs on the electronic structure of monolayer MoS₂ using density functional theory, considering ideal oxides and MoS₂ layers, as well as those with near-interface O vacancies in the oxide slab, or Mo or S vacancies in the MoS₂ layer. Band structures and atom-projected densities of states for each system and with differing oxide terminations were calculated, as well as those for isolated material layers for reference. Among our results, we find that O-terminated and H-passivated HfO₂ and Al₂O₃ exhibit potential as good substrates or gate insulators for monolayer MoS₂, with a straddling gap energy band alignment for the composite system devoid of any defect states within the band gap of the MoS₂, while Hf-terminated HfO₂ leads to a staggered gap alignment, such that holes would be localized to the oxide rather than the MoS₂ layer. With O vacancies, both the Hf-terminated MoS₂-HfO₂ system, and the O-terminated and H-passivated Al₂O₃-MoS₂ systems appear metallic due to doping of the oxide slab followed by electron transfer into the MoS₂, in manner analogous to modulation doping.

I. INTRODUCTION

The unique electrical and optical properties of monolayer transition metal dichalcogenides (TMDs)^{1,2} have spurred intense research interest towards development of nanoelectronic devices utilizing these novel materials.³⁻⁸ However, the two dimensional (2D) nature of monolayer TMDs makes their properties susceptible to the surrounding environment, as evidenced by the mobility enhancement of monolayer MoS₂ when placed on a high-k dielectric such as HfO₂.^{3,9} Theoretical calculations of HfO₂ interfaces have indicated that band offsets can be altered chemically by utilizing different interface terminations.¹⁰ These results puts into stark focus the need to consider the effect of surrounding materials and the interfaces with them on the characteristics of monolayer TMDs. Here, we study the effect of the dielectric oxides HfO₂ and Al₂O₃, both with and without O vacancies, on the electronic structure of monolayer MoS₂ using density functional theory (DFT).

In this work, two possible terminations for the HfO₂ (Al₂O₃) slab were considered: an O-terminated HfO₂ (Al₂O₃) slab with H passivation, and an Hf (Al)-terminated HfO₂ (Al₂O₃) slab. We calculate the band structure and the atom-projected density of states (AP-DOS) for these systems, and compare them to the results for freestanding monolayer MoS₂. The effects of O-vacancies in the first few layers of oxide on the band structure of the MoS₂-oxide system were also simulated, with results for vacancies in the topmost/MoS₂-adjacent O layer shown here. In a similar vein, we also introduced Mo and S vacancies in MoS₂ monolayer to investigate the corresponding effect on MoS₂-oxide electronic structure.

II. COMPUTATIONAL APPROACH

The DFT calculations were performed using the projector-augmented wave method with a plane-wave basis set as implemented in the Vienna *ab initio* simulation package (VASP).^{11,12} The local density approximation (LDA)¹³ was employed for the exchange-correlation potential as LDA has been shown to reproduce the band gap of monolayer MoS₂ well.¹⁴ The calculated lattice constant after volume relaxation of monolayer MoS₂ is also a good match to the experimental value.¹⁵ In our study, two representative dielectrics HfO₂ (chosen for its high- k value) and Al₂O₃ (minimal lattice mismatch) were considered. The hexagonal MoS₂ monolayer was taken to be unstrained, with a volume-relaxed lattice constant of $a = 3.122$ Å. For the dielectric oxide, the energetically stable crystalline phases of bulk HfO₂ and Al₂O₃ at ambient conditions, namely, monoclinic HfO₂¹⁶ and hexagonal Al₂O₃¹⁷, respectively, were utilized.

Our simulations were performed by constructing a supercell of monolayer MoS₂ on an approximately 2 nm thick oxide slab. For HfO₂, atomic relaxation was performed within a rectangular supercell ($a = 9.366$ Å, $b = 5.407$ Å) chosen to reduce the lattice mismatch between monolayer MoS₂ and monoclinic HfO₂. However, a roughly 6% strain remains along the in-plane directions in the HfO₂ (Fig. 1(a)); the MoS₂ layer of principle interest was held as unstrained. For Al₂O₃, atomic relaxation was performed in a (rotated) hexagonal supercell ($a = 8.260$ Å) with a strain of only about 0.2% (Fig. 1(b)). The systems were relaxed until the Hellmann-Feynman forces on the atoms were less than 0.02 eV/Å. During relaxation, all the MoS₂ monolayer atoms and the top half of the layers of the dielectric oxide were allowed to move in the three dimensions. Oxygen vacancies were modeled by removing a single O atom from an O-layer of the supercell. Since we have periodic supercells, the O vacancy is repeated in each instance of the supercell. The system is then allowed to relax again with the introduced O-vacancy. A similar procedure was followed in the modeling of Mo and S vacancies in the MoS₂-

HfO₂ system. In the latter case, the S atom vacancy was introduced in the layer adjacent to the oxide surface. All simulations were performed at a temperature of 0 K.

III. RESULTS AND DISCUSSION

The band structure and atom-projected density of states (AP-DOS) have been calculated for the monolayer MoS₂-oxide system considering different possible terminations of the oxide at the interface and including the effect of vacancies in the oxide and MoS₂. We compared (overlaid) the results for the ideal MoS₂-oxide systems to those for freestanding monolayer MoS₂, and the results for the systems with O vacancies to the ideal MoS₂-oxide results. In all cases, the highest occupied state serves as the 0 eV reference energy for the band structure of interest in these 0 K simulations. The reference band structures, however, are shifted up or down to provide a rough fit to the former in terms of band structure and the AP-DOS of the Mo and S atoms.

The simulated band structure of monolayer MoS₂ on O-terminated HfO₂ with H-passivation is shown in Fig. 2(a) (solid black lines). The band structure of free-standing MoS₂ is provided for reference (red dashed lines). Since a rectangular supercell was used in these simulations of MoS₂ on HfO₂, the corresponding Brillouin zone (BZ) is smaller and the K point of the primitive unit cell—where the monolayer MoS₂ band edges are located—folds into the Γ point in the supercell's BZ. The O-terminated and H-passivated HfO₂ has little effect on the band structure of monolayer MoS₂. The band gap is devoid of any defect states, suggesting the potential for HfO₂ to act as an excellent gate insulator or substrate. In addition, the direct band gap is preserved, which is crucial for optoelectronic applications. The absence of band gap states

also is reflected in the AP-DOS for the system (Fig. 2(b)). The AP-DOS also indicates a straddling gap (Type-1) band alignment between the MoS₂ and the HfO₂.

In contrast, our results indicate a significant reduction in the effective band gap of the combined Hf-terminated HfO₂ slab-MoS₂ system (energy gap E_g of approximately 0.9 eV) as compared to that of freestanding monolayer MoS₂, although a direct band gap is preserved (Fig. 3(a)). The lower portion of what otherwise would be the band-gap is filled with states arising from the contribution of Hf and O atoms, as shown in the AP-DOS of Fig. 3(b). Indeed, there now appears to be a staggered gap (Type II) alignment, where holes would be localized in the HfO₂ instead of the MoS₂ layer.

When an O vacancy is introduced into the top layer of the O-terminated and H-passivated HfO₂ slab, in these 0 K simulations, an occupied defect state (band) is introduced within the band gap of monolayer MoS₂ (Fig. 4(a)), which is associated primarily with Hf atoms in the oxide. Analogous Hf-associated defect states also arise in an isolated O-terminated and H-passivated HfO₂ slab (Fig. 5(a) and (b)). In this latter case (and for analogous cases below) we simply removed the MoS₂ layer from the combined system, while otherwise holding the crystal structure fixed as a control. However, the close proximity of the occupied defect band to the conduction band (of the primary or reference band structure) suggests that these states might be able to act as donors. However, the defect band formation due to the limited supercell size and associated very large ($1.974 \times 10^{14}/\text{cm}^2$) O-vacancy density in these simulations leaves the binding energy for lower defect densities uncertain. Alternatively, these interface states could function as relatively shallow charge traps, leading to degradation of device performance.

In the case of Hf-terminated HfO₂-MoS₂ system with an O vacancy in the top layer of oxide, a straddling gap alignment is now produced, as seen in the AP-DOS (Fig. 6(b)) for this

large O-vacancy density, much as for O-terminated HfO_2 . Moreover, there are now two partially occupied bands at the conduction band edge (Fig. 6(a)), both of which are largely localized to the MoS_2 layer, resulting in a system that now appears metallic. Calculation of the band structure for a freestanding Hf-terminated HfO_2 slab with an O vacancy exhibits occupied conduction band edge state associated with the Hf atoms (Fig. 7(a) and (b)). In the combined HfO_2 - MoS_2 system, these electrons are then transferred into the lower conduction-band-edge MoS_2 layer, in a modulation-doping-like process.

Turning to the Al_2O_3 -monolayer MoS_2 system(s), our simulations of monolayer MoS_2 on O-terminated Al_2O_3 with H-passivation again produced a straddling-gap band alignment with a band gap devoid of defect states and minimal effect on the conduction bands of MoS_2 (Fig. 8(a)). With the employed hexagonal supercell, the BZ retains the inherent hexagonal symmetry and the band edges for the system remain at the K point. However, unlike for the HfO_2 case, the valence band near the Γ point is shifted up towards the band edge by a small amount due to mixing of O, Mo and S atom states near 0 eV, as shown in the AP-DOS plot of Fig. 8(b).

In contrast to the corresponding case for the Hf-terminated HfO_2 system, the Al-terminated Al_2O_3 slab-monolayer MoS_2 system retains a straddling gap alignment, (Fig. 9(b)), with some spill over into the nearby surface O states. However, the valence band near the Γ point is lifted above that at the K-point, making the system indirect (Fig. 9(a)). The greater shift can be attributed to the stronger mixing of O atoms with Mo and S atoms, as supported by the larger DOS for the O atoms near 0 eV (Fig. 9(b)).

For the O-terminated and H-passivated Al_2O_3 - MoS_2 system, creation of an O vacancy in the top O-layer of Al_2O_3 introduces a new partially-filled band at the edge of the MoS_2 conduction band (Fig. 10(a)), which is largely localized to the MoS_2 layer (Fig. 10(b)), resulting

in a system that now appears metallic, much as for the Hf-terminated HfO₂-MoS₂ system with an O vacancy. Calculation of the band structure for an isolated O-terminated Al₂O₃ slab with an O vacancy exhibits occupied conduction band edge state associated with the O atoms (Fig. 11(a) and (b)). In the combined Al₂O₃-MoS₂ system, these electrons again are transferred into the lower conduction-band-edge MoS₂ layer, in a modulation-doping-like process.

For Al-terminated Al₂O₃-MoS₂ system, the system retains a straddling gap alignment after the introduction of an O vacancy in the oxide layer. However, an occupied state (band) deep in the band gap of the MoS₂ is produced (Fig. 12(a)), which is localized to the Al and O atoms in the oxide layer (Fig. 12(b)). Such defect states could serve as recombination centers or charge traps. In addition, however, a direct band gap is found at these doping concentrations, in contrast to the Al-terminated Al₂O₃-MoS₂ system without an O vacancy.

The effects of Mo and S vacancies on the band structure of the MoS₂ on O-terminated and H-passivated HfO₂ also have been studied. Utilizing the same rectangular supercell as in our other MoS₂-HfO₂ system computations, we introduced a single Mo or S atom vacancy in the supercell, with the S atom vacancy introduced in the layer adjacent to the oxide surface. The corresponding vacancy density is $1.974 \times 10^{14}/\text{cm}^2$ in either case. The resultant band structure and AP-DOS are plotted in Fig. 13 and Fig. 14 for MoS₂-HfO₂ systems with Mo and S vacancies, respectively. In both cases, a straddling gap alignment is retained, but defect states are introduced into the band gap of the MoS₂ that are localized to the MoS₂ layer (Figs. 13(b) and 14(b)). With the Mo vacancy, several states are introduced within the nominal band gap, both occupied and empty, although at this vacancy concentration, the valence band edge is difficult to define (Fig. 13(a)). In the case of S vacancies in the MoS₂ monolayer, there are two

unoccupied defect states (bands) introduced near mid gap, as well as significant distortion of the valence band edge structure at these vacancy concentrations (Fig. 14(a)).

IV. CONCLUSION

In summary, O-terminated and H-passivated HfO_2 and Al_2O_3 exhibit potential as good substrates or gate insulators for monolayer MoS_2 , with a straddling gap band structure for the composite system devoid of any defect states within the band gap of the MoS_2 . However, monolayer MoS_2 on Hf-terminated HfO_2 shows a staggered gap alignment, such that holes would be localized in the oxide rather than the MoS_2 layer. For an Al-terminated Al_2O_3 slab, however, there is again straddling gap alignment to provide localization of holes to the MoS_2 layer, with some spill over into the nearby surface O states. Occupied near-conduction-band-edge states that might function either as donors or shallow traps are introduced in the MoS_2 -oxide system by O vacancies in the O-terminated and H-passivated HfO_2 - MoS_2 system. With O vacancies, both the Hf-terminated HfO_2 - MoS_2 system, and the O-terminated and H-passivated Al_2O_3 - MoS_2 system appear metallic due to doping of the oxide slab followed by electron transfer into the MoS_2 , in manner analogous to modulation doping. In contrast, Mo and S vacancies in MoS_2 monolayer introduces multiple deep defect states in the band gap of MoS_2 , as well as distorting the band edges.

ACKNOWLEDGMENT

This work is supported by SEMATECH, the Nanoelectronics Research Initiative (NRI) through the Southwest Academy of Nanoelectronics (SWAN), and Intel. We thank the Texas Advanced Computing Center (TACC) for computational support.

REFERENCES

- ¹ K.F. Mak, C. Lee, J. Hone, J. Shan, and T.F. Heinz, Phys. Rev. Lett. **105**, 136805 (2010).
- ² A. Splendiani, L. Sun, Y. Zhang, T. Li, J. Kim, C.-Y. Chim, G. Galli, and F. Wang, Nano Lett. **10**, 1271 (2010).
- ³ B. Radisavljevic, A. Radenovic, J. Brivio, V. Giacometti, and A. Kis, Nat. Nanotechnol. **6**, 147 (2011).
- ⁴ Y. Yoon, K. Ganapathi, and S. Salahuddin, Nano Lett. **11**, 3768 (2011).
- ⁵ J. Chang, L.F. Register, and S.K. Banerjee, Appl. Phys. Lett. **103**, 223509 (2013).
- ⁶ B. Radisavljevic, M.B. Whitwick, and A. Kis, ACS Nano **5**, 9934 (2011).
- ⁷ H. Liu and P.D. Ye, IEEE Electron Device Lett. **33**, 546 (2012).
- ⁸ S. Das, H.-Y. Chen, A.V. Penumatcha, and J. Appenzeller, Nano Lett. **13**, 100 (2013).
- ⁹ D. Jena and A. Konar, Phys. Rev. Lett. **98**, 136805 (2007).
- ¹⁰ P.W. Peacock, K. Xiong, K. Tse, and J. Robertson, Phys. Rev. B **73**, 075328 (2006).
- ¹¹ G. Kresse and J. Furthmüller, Phys. Rev. B **54**, 11169 (1996).
- ¹² G. Kresse and J. Furthmüller, Comput. Mater. Sci. **6**, 15 (1996).
- ¹³ J.P. Perdew and Y. Wang, Phys. Rev. B **45**, 13244 (1992).
- ¹⁴ J. Chang, L.F. Register, and S.K. Banerjee, J. Appl. Phys. **115**, 084506 (2014).
- ¹⁵ T. Böker, R. Severin, A. Müller, C. Janowitz, R. Manzke, D. Voß, P. Krüger, A. Mazur, and J. Pollmann, Phys. Rev. B **64**, 235305 (2001).
- ¹⁶ J. Kang, E.-C. Lee, and K.J. Chang, Phys. Rev. B **68**, 054106 (2003).
- ¹⁷ S.-D. Mo and W.Y. Ching, Phys. Rev. B **57**, 15219 (1998).

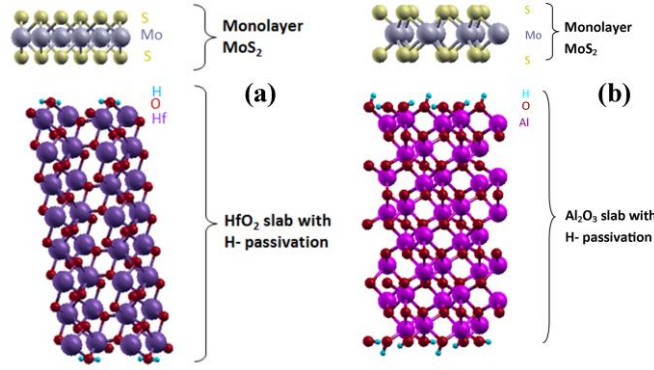


FIG. 1 (color online). (a) Supercell of monolayer MoS₂ on an H-passivated, O-terminated HfO₂ slab of approximately 2 nm thickness (side view). (b) Supercell of monolayer MoS₂ on an H-passivated, O-terminated Al₂O₃ slab of approximately 2 nm thickness (side view).

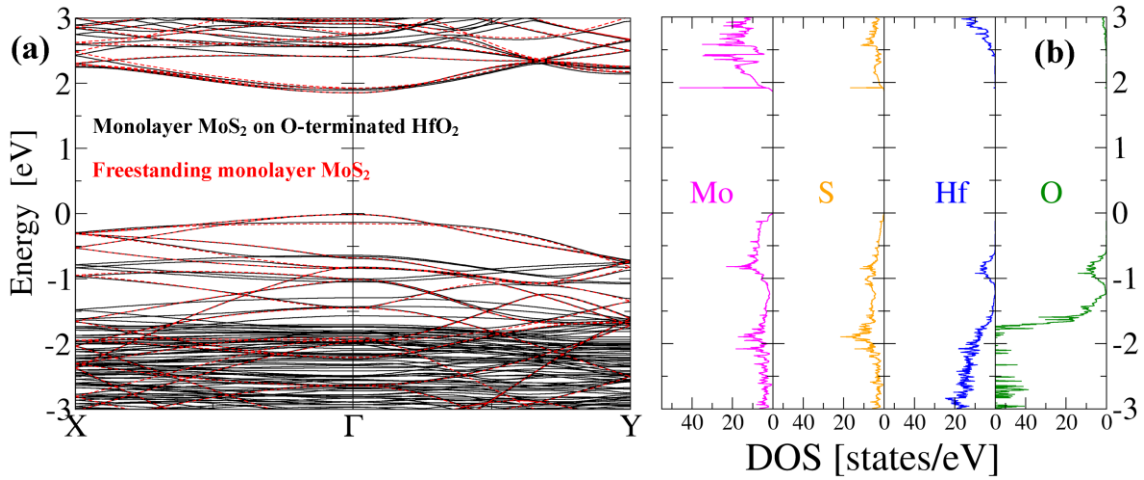


FIG. 2 (color online). (a) Band structure of monolayer MoS₂ on an O-terminated HfO₂ slab with H passivation, plotted along the high symmetry directions of the BZ (black solid lines). The 0 eV reference corresponds to the highest occupied state in these 0 K simulations. The band structure of freestanding monolayer MoS₂ is superimposed for comparison (red dashed lines). This latter band structure, however, is shifted up or down to provide a reasonable fit to the former. (b) Atom-projected density of states (AP-DOS) per eV per supercell for the monolayer MoS₂ and O-terminated HfO₂ system. A straddling gap alignment is observed, devoid of defect states.

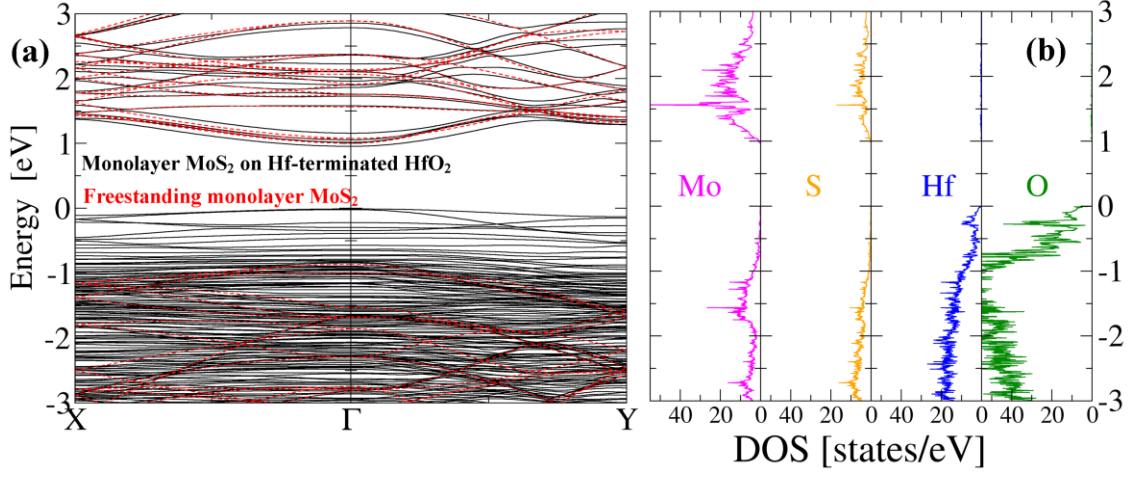


FIG. 3 (color online). (a) Band structure of monolayer MoS_2 on Hf-terminated HfO_2 slab, plotted along the high symmetry directions of the BZ (solid black lines). The band structure of freestanding monolayer MoS_2 is superimposed for comparison (red dashed lines). The reference band structure is shifted up or down to provide a reasonable fit to primary band structure. (b) Atom-projected density of states (AP-DOS) for the monolayer MoS_2 and Hf-terminated HfO_2 system. A staggered gap alignment is observed, such that holes would be localized in the oxide layer rather than the MoS_2 .

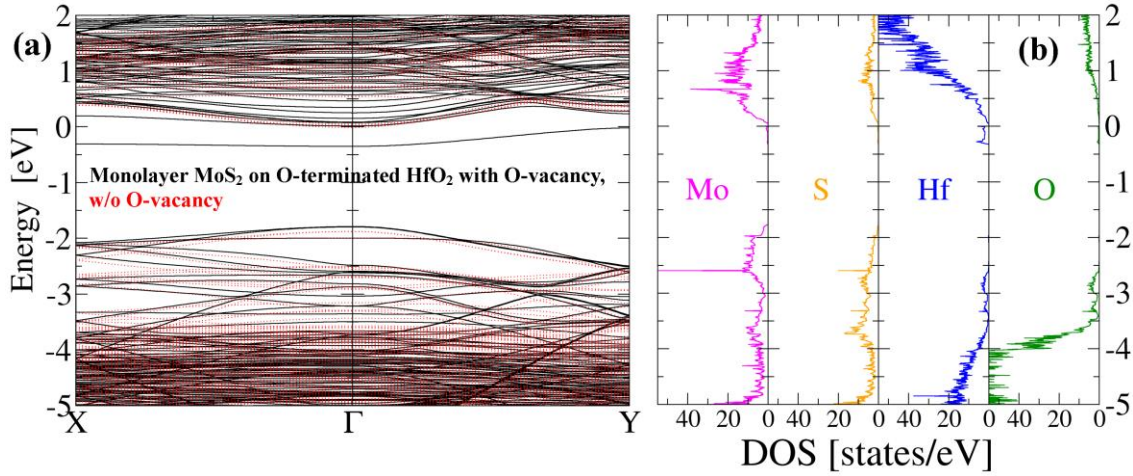


FIG. 4 (color online). (a) Band structure of monolayer MoS_2 on an H-passivated, O-terminated HfO_2 slab with an O-vacancy in the top layer, plotted along the high symmetry directions of the BZ (black solid lines). The band structure of vacancy-free monolayer MoS_2 - HfO_2 system (O-terminated) is superimposed for comparison (red dashed lines). (b) Atom-projected density of states for the monolayer MoS_2 and O-terminated HfO_2 system with an O-vacancy. An occupied defect state (band) is introduced within the band gap of monolayer MoS_2 .

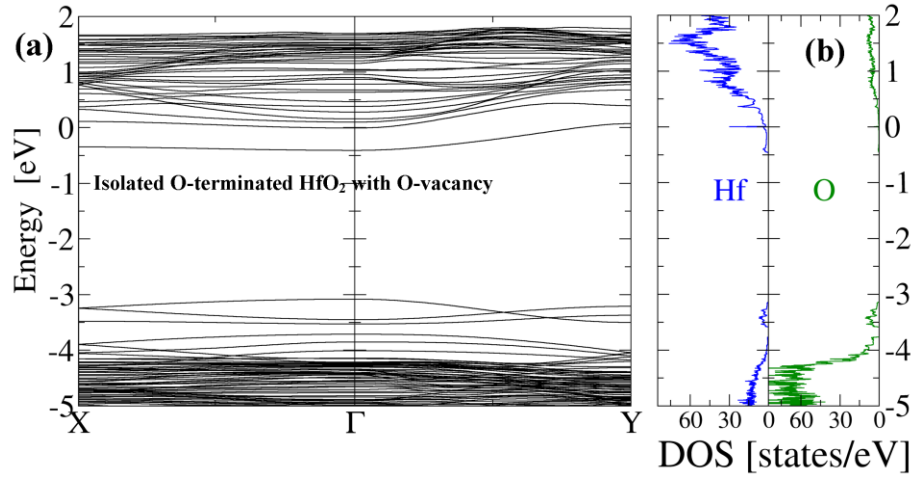


FIG. 5 (color online). (a) Band structure of a freestanding H-passivated, O-terminated HfO_2 slab with an O-vacancy in the top layer, plotted along the high symmetry directions of the BZ. (b) Atom-projected density of states for the O-terminated HfO_2 system with an O-vacancy. Defect states associated with Hf-atoms are observed.

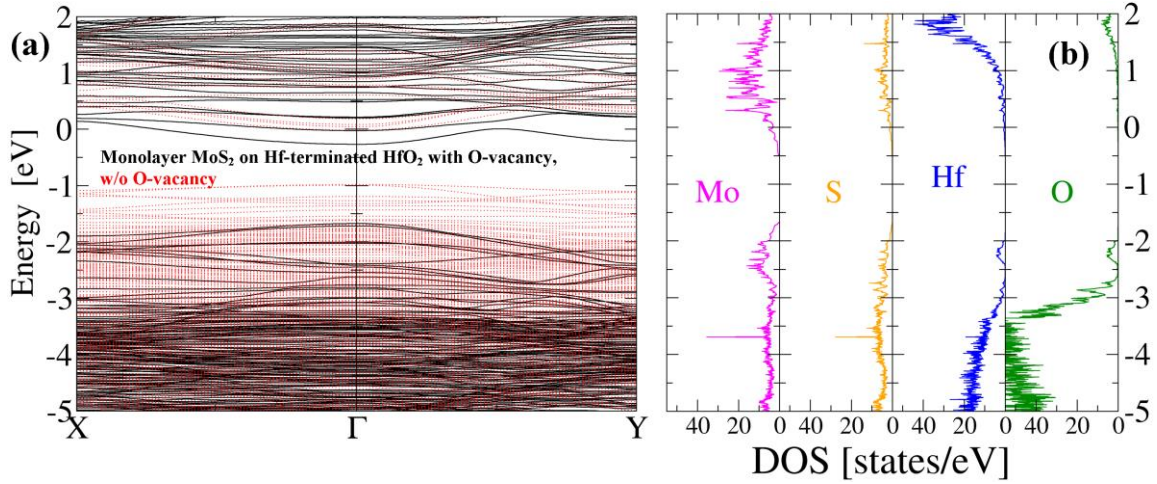


FIG. 6 (color online). (a) Band structure of monolayer MoS_2 on Hf-terminated HfO_2 slab with an O-vacancy in the top layer, plotted along the high symmetry directions of the BZ (black solid lines). The band structure of vacancy free monolayer MoS_2 - HfO_2 system with Hf-termination is superimposed for comparison (red dashed lines). (b) Atom-projected density of states for the monolayer MoS_2 and Hf-terminated HfO_2 system with an O-vacancy. A straddling gap band alignment is now observed along with two partially occupied bands at the conduction band edge both of which are largely localized to the MoS_2 layer, resulting in a system that now appears metallic.

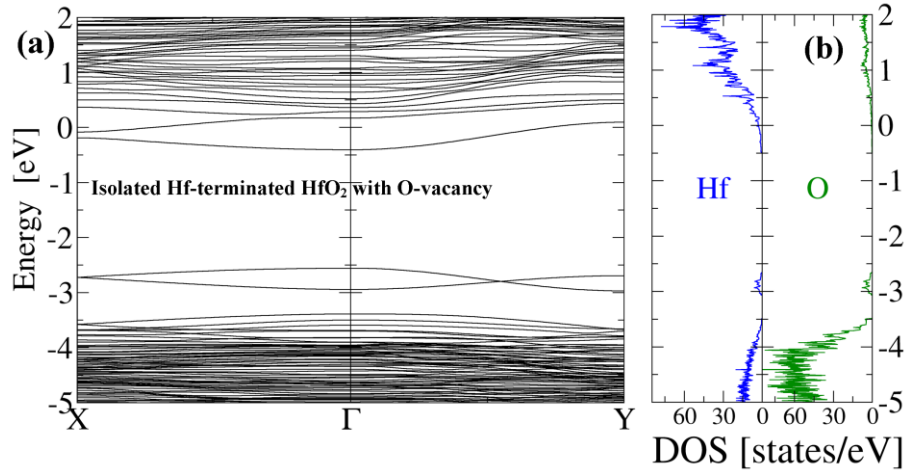


FIG. 7 (color online). (a) Band structure of a freestanding Hf-terminated HfO_2 slab with an O-vacancy in the top layer, plotted along the high symmetry directions of the BZ. (b) Atom-projected density of states for the Hf-terminated HfO_2 system with an O-vacancy. An occupied conduction band edge state associated with the Hf atoms is observed.

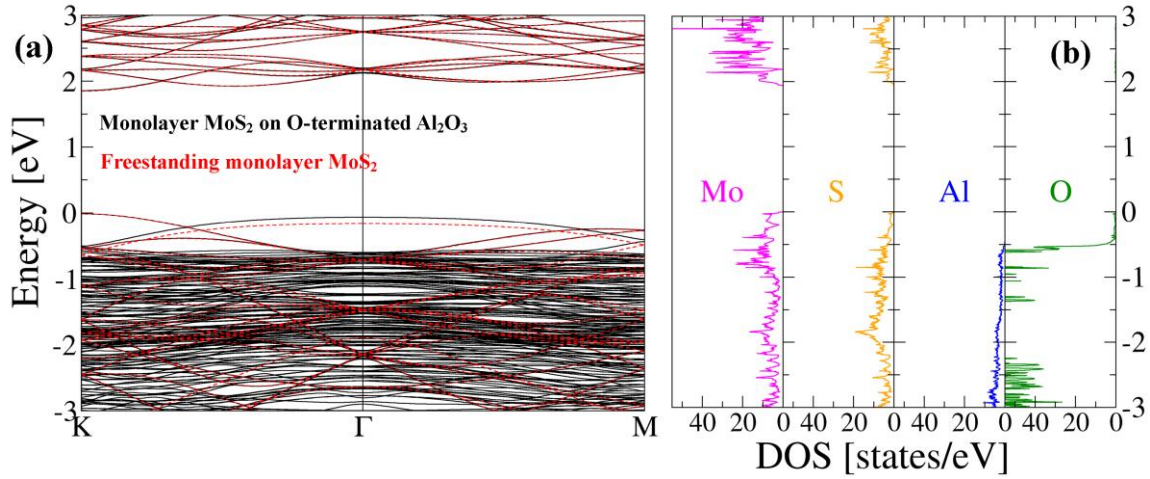


FIG. 8 (color online). (a) Band structure of monolayer MoS_2 on an O-terminated Al_2O_3 slab with H-passivation, plotted along the high symmetry directions of the BZ (black solid lines). The band structure of freestanding monolayer MoS_2 is superimposed for comparison (red dashed lines). (b) Atom-projected density of states for the monolayer MoS_2 and O-terminated Al_2O_3 system. A straddling-gap band alignment is observed with a band gap devoid of defect states.

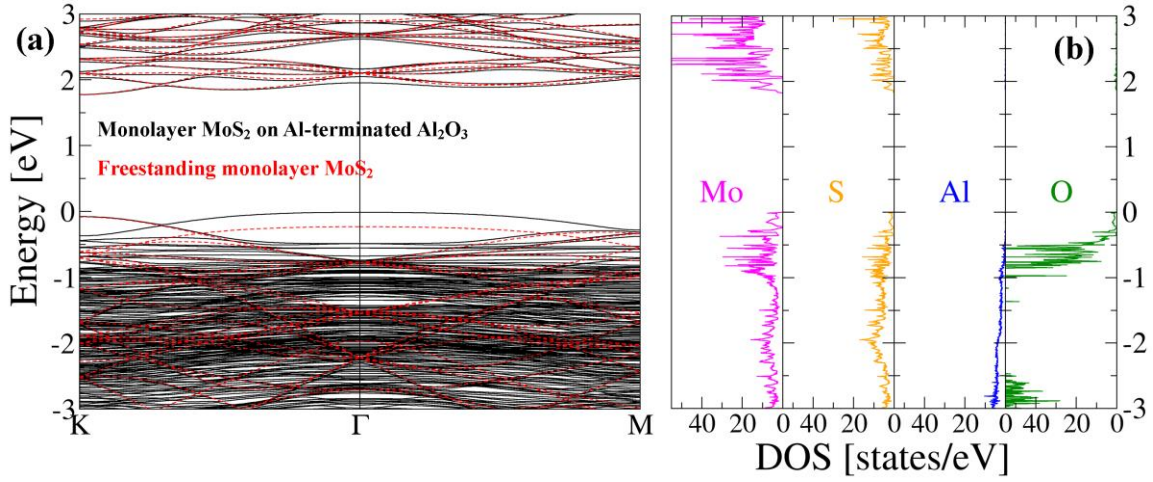


FIG. 9 (color online). (a) Band structure of monolayer MoS₂ on Al-terminated Al₂O₃ slab, plotted along the high symmetry directions of the BZ (black solid lines). The band structure of freestanding monolayer MoS₂ is superimposed for comparison (red dashed lines). (b) Atom-projected density of states for the monolayer MoS₂ and Al-terminated Al₂O₃ system. A straddling-gap band alignment is retained.

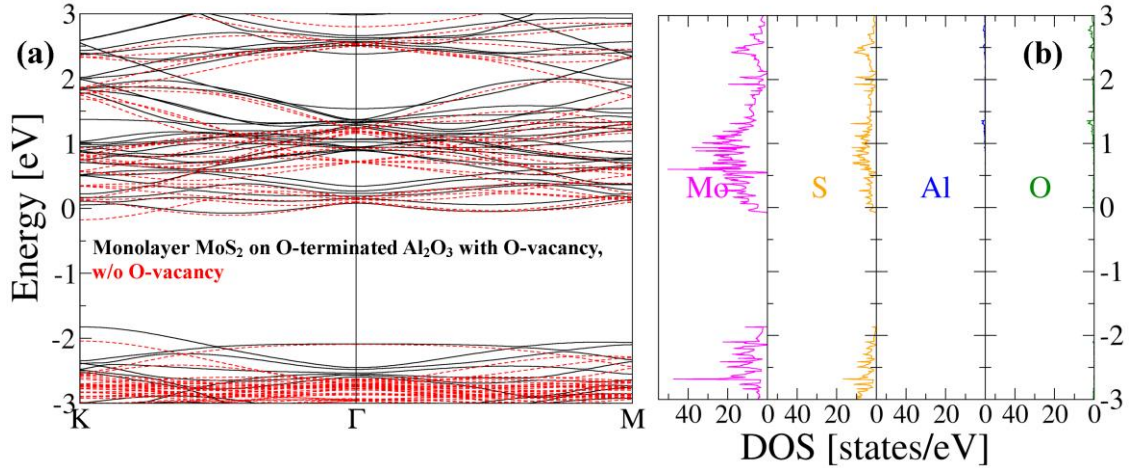


FIG. 10 (color online). (a) Band structure of monolayer MoS₂ on an H-passivated, O-terminated Al₂O₃ slab with an O-vacancy in the top layer, plotted along the high symmetry directions of the BZ (black solid lines). The band structure of vacancy free monolayer MoS₂-Al₂O₃ system (O-terminated) is superimposed for comparison (red dashed lines). (b) Atom-projected density of states for the monolayer MoS₂ and O-terminated Al₂O₃ system with an O-vacancy. A new partially filled band is introduced at the edge of the MoS₂ conduction band, which is largely localized to the MoS₂ layer, resulting in a system that now appears metallic.

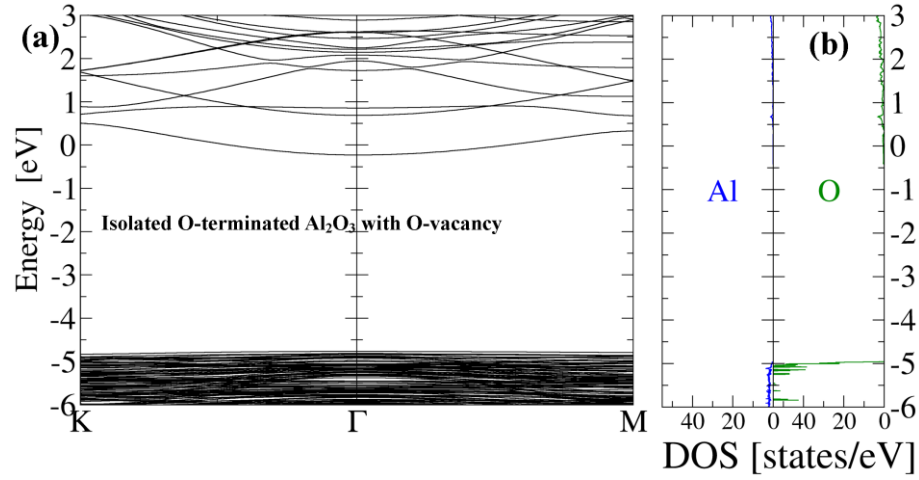


FIG. 11 (color online). (a) Band structure of freestanding H-passivated, O-terminated Al_2O_3 slab with an O-vacancy in the top layer, plotted along the high symmetry directions of the BZ. (b) Atom-projected density of states for the O-terminated Al_2O_3 system with an O-vacancy. An occupied conduction band edge state associated with the O atoms is observed.

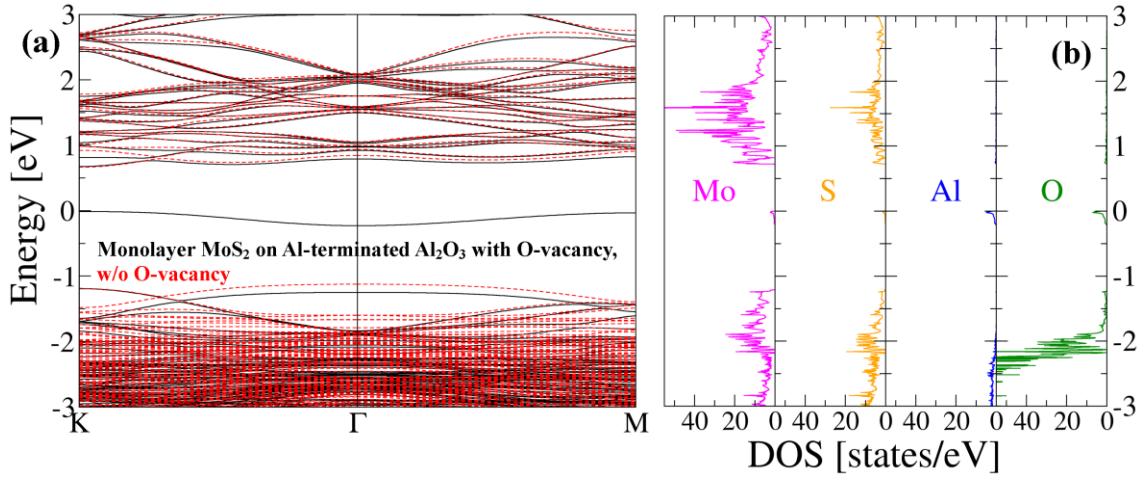


FIG. 12 (color online). (a) Band structure of monolayer MoS_2 on Al-terminated Al_2O_3 slab with an O-vacancy in the top layer, plotted along the high symmetry directions of the BZ (black solid lines). The band structure of vacancy free monolayer MoS_2 - Al_2O_3 system (Al-terminated) is superimposed for comparison (red dashed lines). (b) Atom-projected density of states for the monolayer MoS_2 and Al-terminated Al_2O_3 system with an O-vacancy. An occupied state (band) deep in the band gap of the MoS_2 is produced, which is localized to the Al and O atoms in the oxide layer

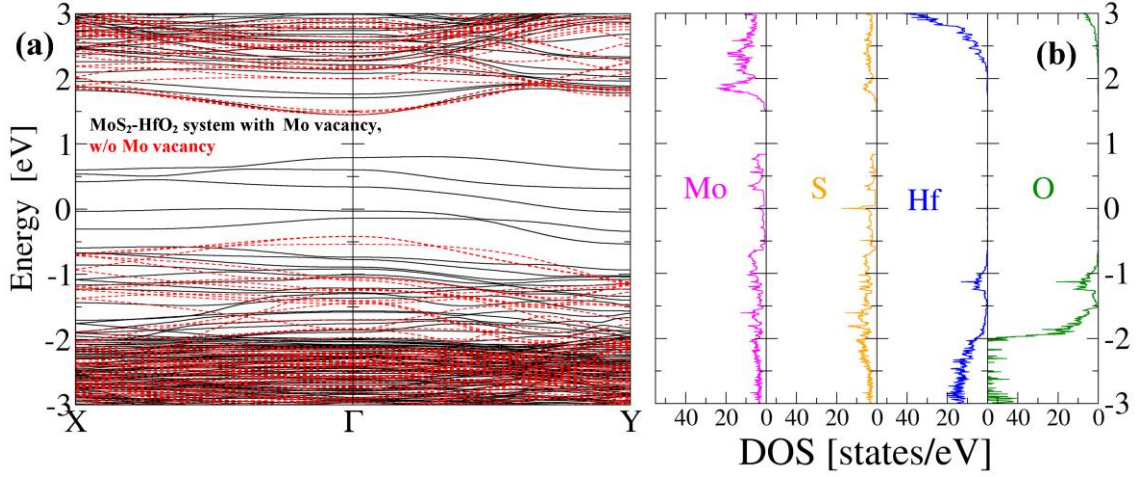


FIG. 13 (color online). (a) Band structure of monolayer MoS_2 on an H-passivated, O-terminated HfO_2 slab with Mo-vacancy in the monolayer, plotted along the high symmetry directions of the BZ (black solid lines). The band structure of vacancy free monolayer MoS_2 - HfO_2 system (O-terminated) is superimposed for comparison (red dashed lines). (b) Atom-projected density of states for the monolayer MoS_2 and O-terminated HfO_2 system with Mo vacancy. Several states are introduced within the nominal band gap and significant distortion of the valence band edge structure is observed.

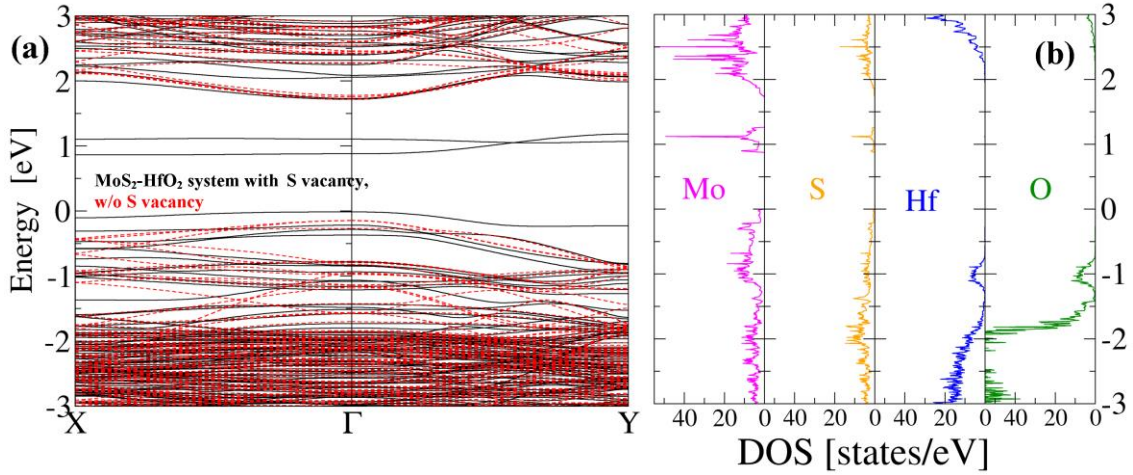


FIG. 14 (color online). (a) Band structure of monolayer MoS_2 on an H-passivated, O-terminated HfO_2 slab with S-vacancy in the monolayer, plotted along the high symmetry directions of the BZ (black solid lines). The band structure of vacancy free monolayer MoS_2 - HfO_2 system (O-terminated) is superimposed for comparison (red dashed lines). (b) Atom-projected density of states for the monolayer MoS_2 and O-terminated HfO_2 system with S vacancy. Two unoccupied defect states (bands) are introduced near mid gap, and significant distortion of the valence band edge structure is observed.